Biophysical Chemistry 197 (2015) 10–17

Contents lists available at ScienceDirect

Biophysical Chemistry

journal homepage: http://www.elsevier.com/locate/biophyschem

On the roles of the alanine and serine in the β-sheet structure of fibroin

Juan Francisco Carrascoza Mayen *, Alexandru Lupan, Ciprian Cosar, Attila-Zsolt Kun, Radu Silaghi-Dumitrescu

Department of Chemistry and Chemical Engineering, "Babes-Bolyai" University, 11 Arany Janos Str, Cluj-Napoca RO-400028, Romania

HIGHLIGHTS

- Semiempirical MP6, DFT calculations and molecular dynamics calculations on fibroin type models are provided.
- These results show how alanine and serine impact the rigidity of β-sheet structures.
- Alanine adds stability to the rigidity of the sheet, allowing it to maintain a properly pleated structure even in a single β-sheet.
- The role of the serine is proposed to involve modulation of the hydrophobicity.

GRAPHICAL ABSTRACT

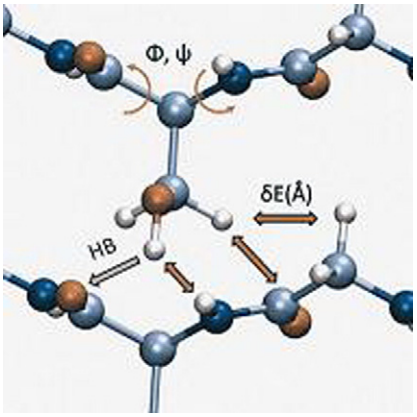

ARTICLE INFO

Article history:
Received 10 June 2014
Received in revised form 20 October 2014
Accepted 9 November 2014
Available online 15 November 2014

Keywords:
Fibroin
Silk II
Molecular modeling
β-sheet
Semiempirical
DFT

ABSTRACT

In its silk II form, fibroin is almost exclusively formed from layers of β-sheets, rich in glycine, alanine and serine. Reported here are computational results on fibroin models at semi-empirical, DFT levels of theory and molecular dynamics (MD) for $(Gly)_{10}$, $(Gly–Ala)_5$ and $(Gly–Ser)_5$ decapeptides. While alanine and serine introduce steric repulsions, the alanine side-chain adds to the rigidity of the sheet, allowing it to maintain a properly pleated structure even in a single β-sheet, and thus avoiding two alternative conformations which would interfere with the formation of the multi-layer pleated-sheet structure. The role of the serine is proposed to involve modulation of the hydrophobicity in order to construct the supramolecular assembly as opposed to random precipitation due to hydrophobicity.

© 2014 Elsevier B.V. All rights reserved.

1. Introduction

Fibroin is a protein rich in glycine, alanine and serine. The "Silk I" conformation of fibroin is known to be relatively flexible, and to rely significantly on intramolecular hydrogen bonds, somewhat reminiscent of collagen, with repeated β-turn motifs [1–3]. This conformation would prevail while fibroin is still within the gland of the worm. By contrast, the "silk II" conformer is more stable, and is known to rely on inter-strand hydrogen bonds between β-strands organized in multiple layers, as illustrated in Fig. 1 [1,2]. The transition from I to II was shown to depend on external factors such as tensile stress and hydration [2–5]. Local β-helix arrangements were also proposed in fibroin [6].

* Corresponding author at: Department of Chemistry and Chemical Engineering, "Babes-Bolyai" University, 11 Arany Janos Str, Cluj-Napoca RO-400028, Romania. Tel.: +40 26 4593833; fax: +40 26 4590818.
E-mail address: carrascoza@chem.ubbcluj.ro (J.F. Carrascoza Mayen).

http://dx.doi.org/10.1016/j.bpc.2014.11.001
0301-4622/© 2014 Elsevier B.V. All rights reserved.

The natural occurrence of the amino acids in silk II involves a ratio of 3:2:1 which can be reflected for instance into a sequence of the type $(Ala–Gly)_2–Ser–Gly$ [1].

Using NMR and empirical calculations, it was shown that alanine protons are engaged in stronger, more favorable inter-strand hydrogen bonds in silk II, as compared to glycine [7]. Computational DFT data have been employed for comparing with the experimental NMR data; notably, the geometries for such DFT computations were built directly to the desired conformations, rather than optimized [8].

With $(AG)_{15}$ peptides, mixtures of β-turns and β-sheets were demonstrated using NMR spectra, with evidence for lamellar arrangements in solution [9,10]. Introduction of serine residues into such AG polypeptides was found to provide even better similarity with fibroin; the role of the serine was proposed to involve loosening of the inter-plane interactions by means of its bulkier and more hydrophilic side-chain [10]. Molecular mechanics and dynamics calculations have been used to describe the folding of both silk I and silk II, and the instability of its aggregated states also followed by NMR data [4]. Buehler and Keten have employed molecular mechanics to show that poly-alanine structures are more likely to engage in crystalline-like β-sheet domains than the glycine rich structures, these authors also evidenced a role for each type of structure under mechanical stress in fibroin [11,12]. This was in line with experimental data showing that in $[GAGAGX]_{16}$ peptides the nature of the amino acid X (A, S, Y or V) has a measurable influence on the ability of the peptide to form β-sheets [13].

Using a small two-peptide model Asakura and co-workers in 2004 [14] applied molecular mechanics in order to show possible ways in which a tyrosine residue may be accommodated within fibroin. With such models, they further described silk I type of structures in water. The position of the tyrosine as an (AG) polypeptide was found to affect the preference for silk II [15] versus silk I conformations [16]. Zhou and co-workers have additionally shown that this tyrosine can yield a spectroscopically detectable free radical, whose signal would be diagnostic between the I and II types of silk [17].

Stewart [18] has shown that semiempirical methods may reasonably describe β-sheet structures in globular-type proteins without stacked sheets of β-strands; tensile strength parameters were then derived from a fibroin model using such semiempirical strategy, although the detailed structure of the optimized geometry has not been discussed [18]. Several studies have shown that the hydrogen bonding interactions within β-sheets are cooperative with contributions to the energy of binding from several layers [19–24].

Molecular dynamics (MD) studies has been used before to obtain information on how the molecular interactions can be understand at atomic level and draw conclusions on the final effect in the structure [25].

We have recently provided an extended analysis of computational methods for predicting another secondary structure element in proteins, the α helix [26]. Here, we report computational data on fibroin using two of the best performing methods for the task, namely PM6 and M06-2x, which were used to compute the energy of interaction between strands, after optimization. We also applied molecular dynamics methods to obtain statistically representative geometrical models and understand its interaction and stability across the time. These data allow not only the estimation of preferred geometries for fibroin-like peptides, but also of the relative energies of interactions, thus allowing formulation of conclusions on the roles of alanine and serine in fibroin. As glycine contains the smallest side-chain, we perform calculations on Gly–Gly multimers as reference, thereafter examining the effect of different side-chains with Gly–Ala and Gly–Ser peptide models.

2. Methods

Polypeptide models were built as ten — amino acid monomer units using the Spartan software package [27] and multiplied up to eighteen such units (6 × 3 monomers) as described previously. Parallel as well as antiparallel structures were considered; however, unless otherwise specified, only antiparallel structures are discussed in Section 3, in line with experimental data [4]. Within a plane each monomer was arranged so that its side-chains point on the opposite side of the layer's plane, relative to the side-chains of the two neighboring-sheets.

Regarding the construction of the layers, we study first a single decapeptide and its relationship with the solvent, then a dimer (non-covalent association of two decapeptides in antiparallel pleated beta sheet conformation) in order to explore chain to chain and dimer–solvent interactions. Subsequently, models of 4 and 6 monomers were done with the intention to observe the systematic effect of isolation of the central

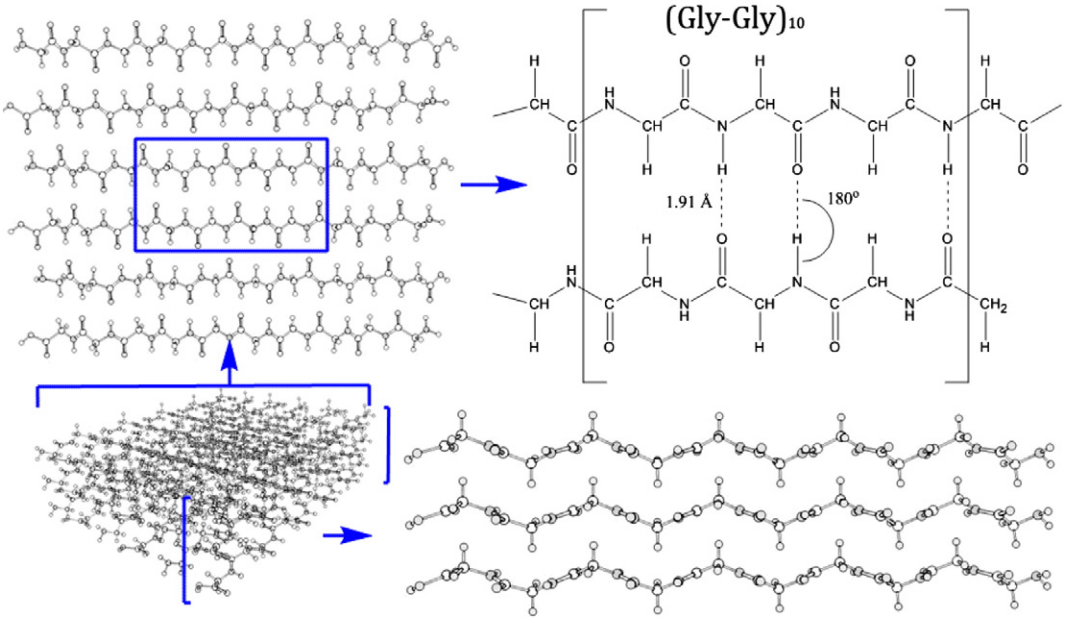

Fig. 1. Assemblies of octadecamers in β-sheets (decaglycine chosen for illustration only) organized canonically according to a putative fibroin-like silk II structure. The $[(Gly–Ala)_5]_{18}$ and $[(Gly–Ser)_5]_{18}$ assemblies are presented in the Supporting Information.

chains into a single layer, but preserving the solvent interaction over and under the layer. Models consisting of 8 and 18 monomers, respectively, were constructed in 3 layers of 2 and 6 monomers each, where we focus our attention over the two central monomers which are isolated from water to observe its interaction only within the polymeric environment. For such structures we analyze the effect of the solvent by MD. This series of models allows one to verify the extent to which the observed trends are systematic, and to explore their size-dependence, thus giving further weight to the conclusions drawn on the largest of the models.

Geometry optimization was performed on all the initial structures, and the results are presented in Fig. 2 and Table 1; the semi empirical PM6-D2 method [28] and CPCM continuous solvent model [29] were employed as implemented in MOPAC 2009 [30,31]; The limited memory BGFS function optimizer, which calculates the hessian as needed, was employed because of the size of some of the systems calculated; the augmented dispersion correction term version 2 (D2) was also taken into account; Localized Molecular Orbital method (MOZYME) algorithm was employed to speed up the SCF iterations; and the solvent effect was induced by simulating water with an effective radius of the solvent of 1.3 Å, electrostatic potential of 78.39 and using Cartesian coordinates to perform the calculations. No hydrogen bond polarization was taken into account. The choice for this methodology was based on recent technical evaluations of the various optimization algorithms of the PM6 method in the MOPAC2009 software package on various polypeptides [26,32]. Convergence was reached when the default SCF criterion of 1×10^{-4} kcal/mol was achieved and the Herbert test was satisfied as performed by default within MOPAC.

As reference, DFT geometry optimizations on single-sheets were performed by using the hybrid meta-GGA functional M06-2X [33] and the 6–31G** basis set as implemented in Gaussian 09 program [34] with standard convergence criteria: the maximum force of the system was set with a threshold of 0.000450 Hartree and a RMS threshold of 0.0003; maximum displacement was set with a threshold of 0.0018 Å and RMS of 0.0012.

Molecular mechanics–molecular dynamics calculations were performed using the Amber14 force field [35,36] as implemented in Sander. MPI program contained in AmberToolkit version 14 [37]. These calculations were performed to analyze the stability of the systems across the time. All the systems were first geometry optimized with PBC conditions of 1 Angstrom distance from all the amino acidic atoms of the system into a cubic box of water, at 300 K and NVT. Then sequenced heating was performed from 0 to 300°K, at NPT conditions, followed by molecular dynamics during 60 fs where SHAKE algorithm [38] was used and no other constrains were imposed. This first 60 fs was discarded to sampling later 5 ns in the same conditions, the results presented in Section 3 were taken from the average of the latest 5 nanosecond time. The Amber14 all atoms force field implements better statistical corrections to avoid over estimation of α-helix conformations although it implements no changes for amino acids since its version Amber10, which results on folding of proteins already has been observed [39].

3. Results and discussion

3.1. Effects of the methodology on the models

We have previously tested several minimization protocols with PM6 with and without correction term variants in α-helix Gly_{10} monomers [32]. PM6 as an ab-initio based method, relies on a Hamiltonian that applies a correction term for energy and considers the hydrogen bond formation as static. In terms of energy the error can be up to 4.44 Kcal/mol [31,32]. To reduce this error, our calculations include a dispersion correction term version 2 (D2) as implemented by MOPAC (c.f. Methodology section), and no polarization of the hydrogen bond was taken into account, because as published by MOPAC developers, the correction term for hydrogen bond polarization gives as result energies of interaction rather than energies of formation.

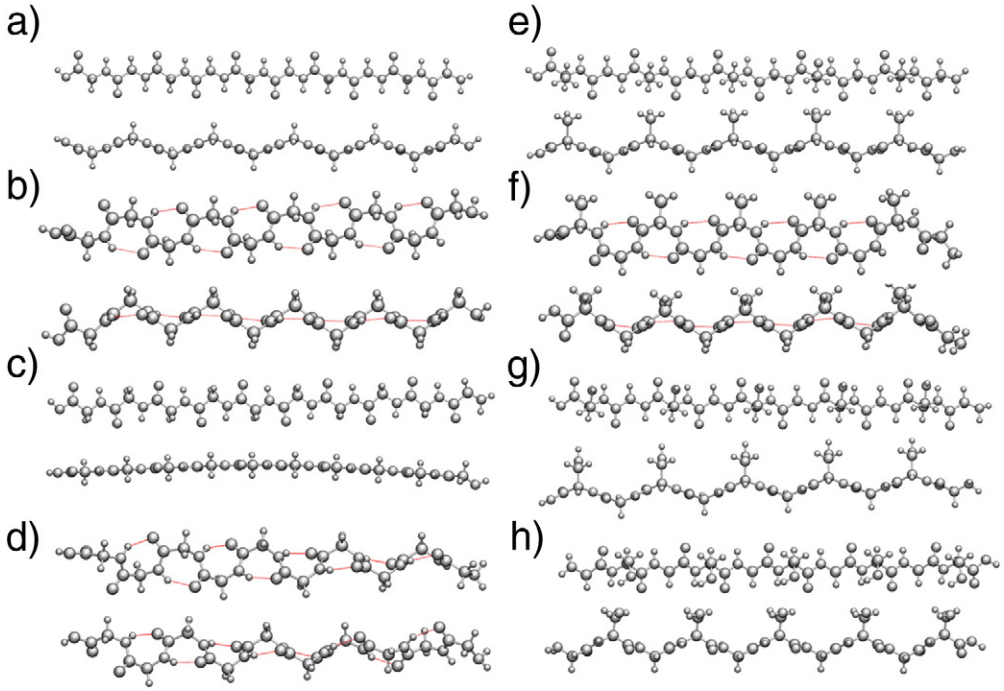

Fig. 2. Gly_{10}, $(Gly–Ala)_5$ and $(Gly–Ser)_5$ decapetides organized as single β-sheets: geometries before and after optimization with DFT (M06-2x/6–31G**) and PM6 methods. Internal hydrogen bonds are indicated with dashed red lines. Top and side views are shown for each structure. a) — Gly_{10} starting geometry. b) — PM6–Gly_{10} optimized. c) — Non-pleated Gly_{10} DFT-optimized. d) — pleated Gly_{10} DFT-optimized. e) — $(Gly–Ala)_5$ starting geometry. f) — $(Gly–Ala)_5$ PM6 optimized. g) — $(Gly–Ser)_5$ starting geometry. h) — $(Gly–Ser)_5$ PM6-optimized.

Table 1
Energies for PM6 optimized models (kcal/mol). Stabilization energies are calculated as the difference between the energy resulted from geometry optimization and the appropriate multiple of the energy obtained by a single point calculation on a single-monomer extracted from the core of a PM6 optimized eighteen-monomer model (references marked with *).

Model	Monomers	Hydrogen bonds	Energy (kcal/mol)	Stabilization energy (kcal/mol)		
				Total	Per amino acid	Per hydrogen bond
$(Gly)_{10}$ *	1	0	−553.1	0.0	0.0	0.0
$(Gly)_{10}$	1	8	−565.1	−12.1	−1.2	−1.5
$[(Gly)_{10}]_2$	2	13	−1135.8	−29.6	−1.5	−2.3
$[(Gly)_{10}]_4$	4	31	−2297.7	−85.3	−2.1	−2.8
$[(Gly)_{10}]_8$	8	60	−4692.7	−267.9	−3.3	−4.5
$[(Gly)_{10}]_6$	6	50	−3460.9	−142.4	−2.4	−2.8
$[(Gly)_{10}]_{18}$	18	156	−10,743.0	−787.9	−4.4	−5.1
$(GlyAla)_5$ *	1	0	−593.2	0.0	0.0	0.0
$(GlyAla)_5$	1	7	−600.9	−7.7	−0.8	−1.1
$[(GlyAla)_5]_2$	2	11	−1215.3	−28.9	−1.4	−2.6
$[(GlyAla)_5]_4$	4	31	−2461.1	−88.3	−2.2	−2.8
$[(GlyAla)_5]_8$	8	61	−4998.2	−252.6	−3.2	−4.1
$[(GlyAla)_5]_6$	6	41	−3706.6	−147.5	−2.5	−3.6
$[(GlyAla)_5]_{18}$	18	150	−11,377.0	−699.4	−3.9	−4.7
$(GlySer)_5$ *	1	1	−793.1	0.0	0.0	0.0
$(GlySer)_5$	1	0	−799.2	−6.1	−0.6	0.0
$[(GlySer)_5]_2$	2	17	−1632.6	−46.4	−2.3	−2.7
$[(GlySer)_5]_4$	4	53	−3302.2	−129.8	−3.2	−2.4
$[(GlySer)_5]_8$	8	95	−6683.4	−338.6	−4.2	−3.6
$[(GlySer)_5]_6$	6	50	−4970.0	−211.3	−3.5	−4.2
$[(GlySer)_5]_{18}$	18	150	−15,210	−933.6	−5.2	−6.2

To assess the theory level effect on geometry of the system, one should take a close look at Fig. 2-B, C and D. Fig. 2-B is the PM6 result, and its conformation is 2.2_7 ribbons, which contains several intrahydrogen bonds. The DFT M06-2x functional, which includes a correction term for hydrogen bonds, has proven to be more accurate for the prediction of biopolymer conformations than other functionals. M06-2x has identified two different conformers: a completely flat β-sheet and a distorted 2.2_7 ribbon conformation very similar to the one obtained by PM6.

The tendency of PM6 calculations to slightly overestimate internal hydrogen bonds over intramonomer hydrogen bonds, is almost negligible in the models containing a larger number of peptide chains (up to 18). The accuracy of the calculated energy of formation by PM6-D2 with L-BGFS in comparison with those obtained by DFT M06-2x suggests that this semiempirical method is indeed appropriate for the study of the much larger models, where DFT would be far less feasible.

3.2. Glycine

PM6 calculations on conformers of the single Gly_{10} decapeptide reveal that the 2.2_7 ribbon is more stable by 12 Kcal/mol than a β-sheet conformation (c.f. Table 1, Fig. 2) — which is entirely expected since a single peptide does not benefit from the intermolecular stabilizing hydrogen bonds that define a pleated β-sheet. Using DFT M06-2x with CPCM solvation in water, two conformations were shown as possible: β-sheet and 2.2_7 ribbon. Fig. 3 illustrates Ramachandran plots for the models mentioned above and the corresponding geometries are shown in Fig. 4. Thus, a single Gly_{10} decapeptide will tend to form 2.2_7 ribbons. This can also be seen in the MD results. Also, the structure searches for less steric hindrance, which for Gly multimers is achieved intercalating the backbones of the monomers across the layers (cf. Fig. 5).

3.3. Alanine

To understand the influence of alanine's methyl group, one may first compare the $[Gly_{10}]_2$ and $[(Gly–Ala)_5]_2$ stabilization energies per hydrogen bond (cf. Table 1); the Gly–Ala structure is better stabilized, by 0.3 Kcal/mol. Arrangements into a single layer but with 4 monomers, $[Gly_{10}]_4$ and $[(Gly–Ala)_5]_4$, gave the same stabilization energy per hydrogen bond, −2.8 kcal/mol. For hexameric models on a single layer, the Gly–Ala structure is again 0.8 Kcal/mol more stable regarding hydrogen bond interactions. However, in models with two layers of β sheets, where side-chain volume intervenes as a steric factor as the alanine methyl group clashes with its upper neighbor, $[Gly_{10}]_8$ is better stabilized than $[(Gly–Ala)_5]_8$: −4.5 vs −4.1 kcal/mol. For $[Gly_{10}]_{18}$ vs $[(Gly–Ala)_5]_{18}$ the energies of stabilization per hydrogen bond are −5.1 and −4.7 kcal/mol, respectively, with a 0.4 Kcal/mol in difference in favor of the Gly–Gly structures.

According to the molecular dynamics results, an observed light distortion in the Gly–Ala octadecamer from a completely flat β-sheet into 2.2_7 ribbon-hybrid shaped pattern may help limit side chain steric clashes (Fig. 6), but it also distorts the hydrogen bonds (third column Table 1, Gly–Gly vs Gly–Ala), therefore making the Gly–Ala sequences mechanically and thermodynamically less favorable, in line with the PM6 geometry optimization results.

However, comparing Gly–Gly vs. Gly–Ala eighteen-mer structures after molecular mechanics–molecular dynamics calculations (MM/MD), Gly–Ala structures show a higher gain of distance of 1.27 Å between up and down monomers (cf. Table 2), meaning that the repulsion and pulling forces in Gly–Ala is stronger. Also, the MD results show that the backbone chains change their zigzag orientation from generally planar sheets in Gly–Gly structures, to the canonical pleated sheets on the other models, due to steric hindrance of the side-chains (Fig. 6).

3.4. Serine

Even in the single decapeptide model, serine leads to a pleated β-sheet conformation (cf. Figs. 3, 1 and 1* monomers). This is not only due to the sterics, but also to the fact that serine provides an extra hydroxyl group that in the pleated conformer is able to engage in hydrogen bonds between the Ser side-chains.

Ser–Ser side-chain hydrogen bonds also occur between monomers within neighboring layers. Indeed, the energy of relative stability due to the hydrogen bond formation was the same when the monomer stands alone or when it is taken from middle of an eighteen-monomer structure (c.f. Table 1). Comparing to Gly–Gly structures, Gly–Ser seems to have a slightly better stability in models consisting of a single

Number of monomers	Gly–Gly	Gly–Ala	Gly–Ser
1*	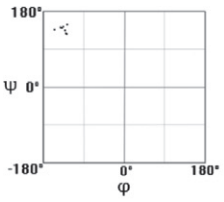	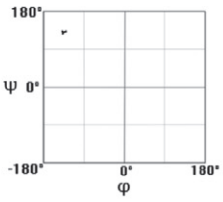	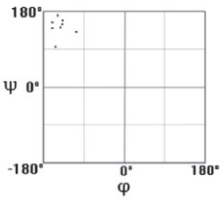
1	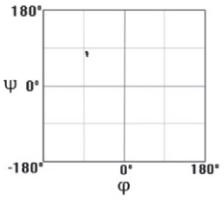	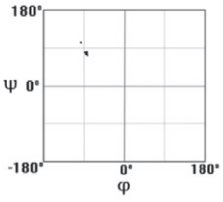	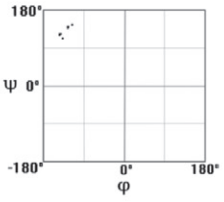
2	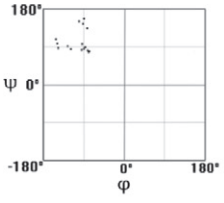	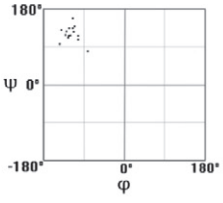	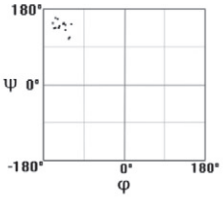
4	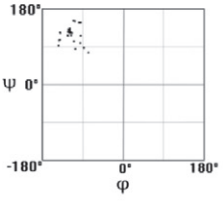	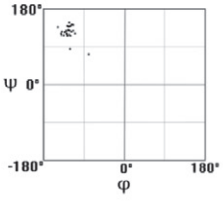	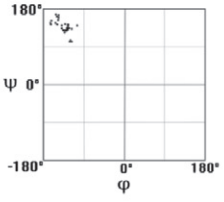
8	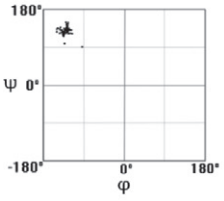	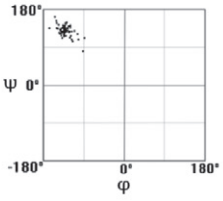	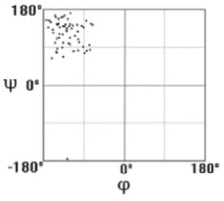
6	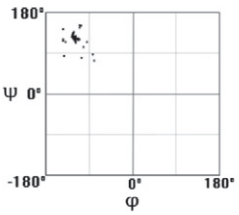	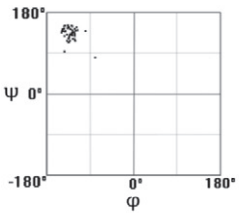	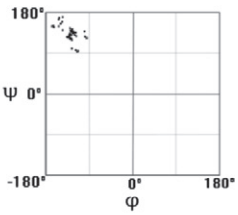
18	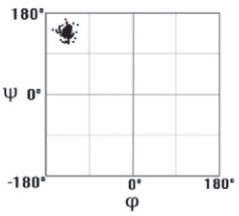	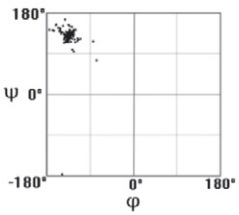	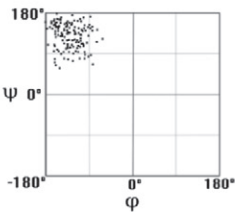

Fig. 3. Ramachandran plots for PM6 results.

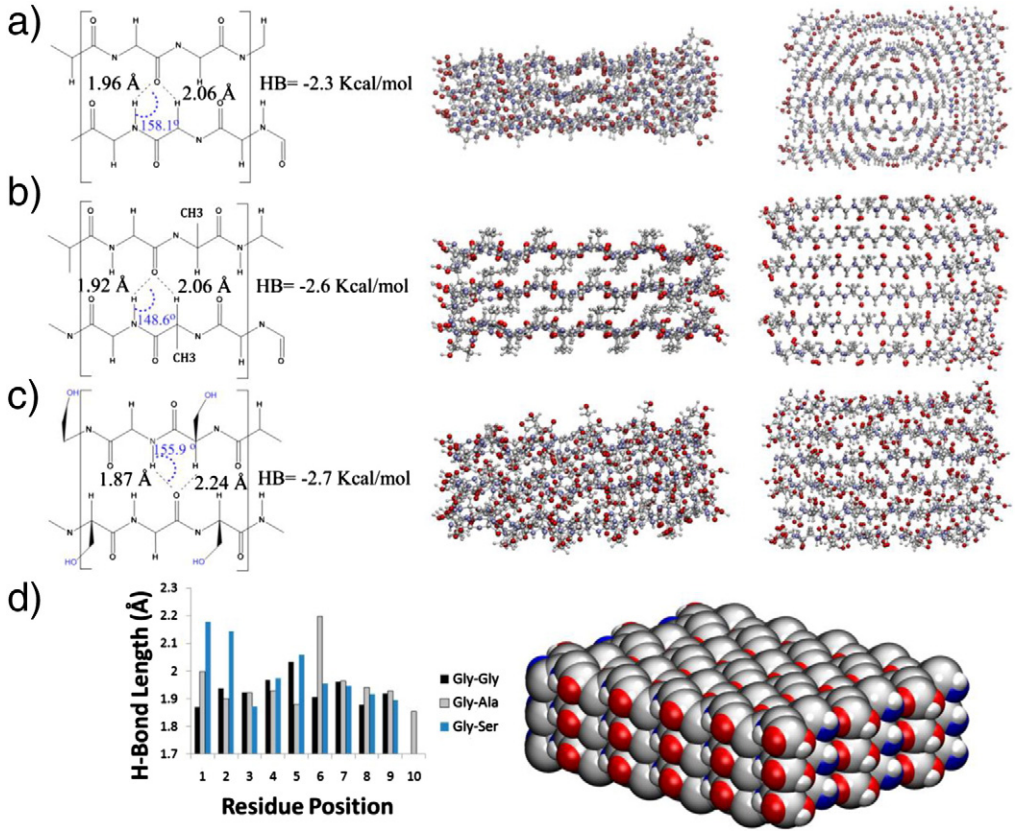

Fig. 4. PM6 optimized geometries of fibroin-like models. Left: hydrogen bond distance, angle and formation energy. Center: lateral view. Right: top view. A. $(Gly_{10})_{18}$ antiparallel E. B. $((Gly–Ala)_5)_{18}$ antiparallel E. C. $((Gly–Ser)_5)_{18}$ antiparallel E. bonds. B. Left. Lengths of hydrogen bonds for a monomer taken from the center of the 18 monomer structure. D. Right: tridimensional model of the octadecamer assembles optimized. Abbreviations: HB: hydrogen bond average energy.

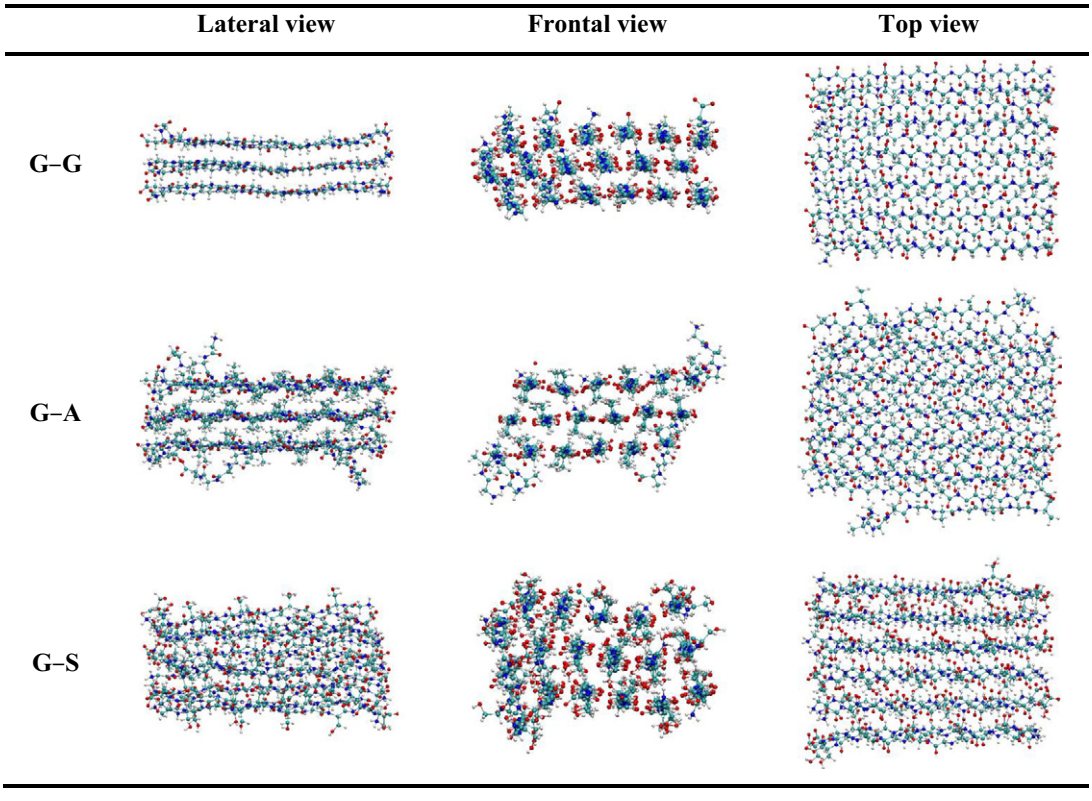

Fig. 5. 18-mer structures after 5 ns of MM/MD.

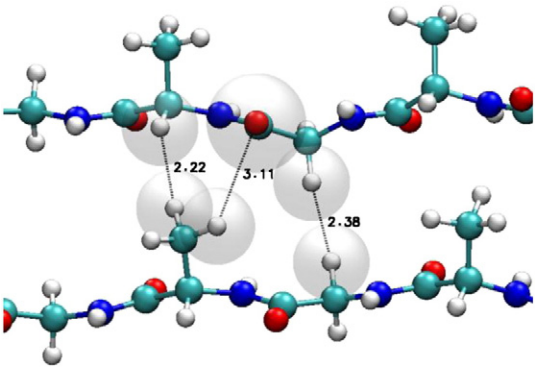

Fig. 6. $[(Gly–Ala)_5]_{18}$ structure. Close up on backbone interactions for a dimer extracted from the eighteen-mer complex after 5 ns of MM/MD. Shown distances of interaction are from a calculated averaged structure, expressed in Angstroms.

layer of β sheets. However, where two or more layers are involved the order is reversed; thus, the relative energy of hydrogen bonds for 8-decapeptide models structured into 3 layers is 1 kcal/mol better for $[(Gly–Gly)_5]_8$.

Comparing Gly–Ser with its homologous Gly–Ala 8-chain structure, the difference is 0.5 Kcal/mol favoring the Gly–Ala structure. This means that the potential contribution of an extra hydrogen bond is compromised against steric hindrance caused by hydroxyl group's volume.

Analyzing the eighteen-monomer structures, Gly–Ser has stabilization energy per amino acid of 1.3 Kcal/mol higher than its homologous Gly–Ala, while Gly–Ser is 0.8 Kcal/mol more stable than Gly–Gly. Therefore, this seems to be the most stable structure (cf. Table 1).

Analyzing the MM/MD results for Gly–Ser eighteen-mer structures, the total energies of these systems follow the same trends as in the PM6 results. The distance between backbones and between hydrogen bonds are the highest too in average (c.f. Table 2). Yet it is also observable through the dynamics that the Gly–Ser structures tends to dissolve easier, meaning that the solvent effect plays an important role due to the hydrophobic R-chain of Ser, as expected. At the same time, the internal monomers of the eighteen-mer structure get contracted.

For all the structures, the solvent effect tends to change the β-sheet conformation to a 2.2_7 ribbon conformation. Between the three types of structures analyzed, Gly–Gly rather preserve its compactness. In Gly–Ala structures the effect was that across the time, and because of the repulsion of the chains plus the solvent effect, the structure tends to be dissolved. Gly–Ser structures tend to be dissolved too, but because of the hydrogen bond formation that is easier due to the R-group of serine.

4. Conclusions

We have reported here on the stabilization energies for inter- and intra-monomer interactions, as well as for interactions between parallel planes, in fibroin models. We find that the role of alanine is to impart rigidity within each pleated-sheet, thus priming it for secondary structure formation with another-sheet; this comes at the expense of a slight destabilization of the interactions between the planes of the fibroin. We find that serine disrupts the multiple-plane, multiple-sheet fibroin structure, and propose that its presence in this protein involves a role in the formation of the more water-soluble silk I form; in the absence of serine, fibroin would be too hydrophobic to be manipulated even at the ribosomal stage.

Table 2
MM/MD averaged results after 5 ns divided into 2500 frames. All the energies are reported in Kcal/mol, and the distances in Angstroms. Further details of the MD calculations can be found in Supporting Information.

18-mer structure	NHB	DHB	DBB
Gly–Gly	107.5	2.00	4.42
Gly–Ala	94.9	1.99	5.69
Gly–Ser	126.4	2.09	5.90

Abbreviations: NHB Number of hydrogen bonds; DHB Average distance computed for the hydrogen bonds; and DBB Distance between backbone α carbons of the β sheet layers.

Acknowledgments

Funding from the Romanian Ministry of Education and Research, (grant PN II 312/2008) is gratefully acknowledged.

Appendix A. Supplementary data

Supplementary data to this article can be found online at http://dx.doi.org/10.1016/j.bpc.2014.11.001.

References

[1] K. Okuyama, R. Somashekar, K. Noguchi, S. Ichimura, Refined molecular and crystal structure of silk I based on Ala–Gly and (Ala–Gly) (2)-Ser–Gly peptide sequence, Biopolymers 59 (2001) 310–319.
[2] T. Yamane, K. Umemura, Y. Nakazawa, T. Asakura, Molecular dynamics simulation of conformational change of poly(Ala–Gly) from silk I to silk II in relation to fiber formation mechanism of *Bombyx mori* silk fibroin, Macromolecules 36 (2003) 6766–6772.
[3] T. Asakura, et al., A repeated beta-turn structure in poly(Ala–Gly) as a model for silk I of *Bombyx mori* silk fibroin studied with two-dimensional spin-diffusion NMR under off magic angle spinning and rotational echo double resonance, J. Mol. Biol. 306 (2001) 291–305.
[4] A. Nagano, Y. Kikuchi, H. Sato, Y. Nakazawa, T. Asakura, Structural characterization of silk-based water-soluble peptides (Glu) n (Ala–Gly–Ser–Gly–Ala–Gly) 4 (n = 4–8) as a mimic of *Bombyx mori* silk fibroin by 13 C solid-state NMR, Macromolecules 42 (2009) 8950–8958.
[5] T. Asakura, J. Yao, M. Yang, Z. Zhu, H. Hirose, Structure of the spinning apparatus of a wild silkworm *Samia cynthia ricini* and molecular dynamics calculation on the structural change of the silk fibroin, Polymer (Guildf) 48 (2007) 2064–2070.
[6] N.D. Lazo, D.T. Downing, Crystalline Regions of *Bombyx mori* Silk Fibroin May Exhibit-Turn and -Helix Conformations, 1999. 4700–4705.
[7] Y. Suzuki, et al., Intra- and intermolecular effects on 1H chemical shifts in a silk model peptide determined by high-field solid state 1H NMR and empirical calculations, J. Phys. Chem. B113 (2009) 9756–9761.
[8] P. Zhou, G. Li, Z. Shao, X. Pan, T. Yu, Structure of *Bombyx mori* Silk Fibroin Based on the DFT Chemical Shift Calculation, 2001. 12469–12476.
[9] T. Asakura, H. Sato, F. Moro, Y. Nakazawa, A. Aoki, Lamellar structure in poly(ala–gly) determined by solid-state NMR and statistical mechanical calculations, J. Am. Chem. Soc. 129 (2007) 5703–5709.
[10] T. Asakura, Y. Nakazawa, E. Ohnishi, F. Moro, Evidence from 13C solid-state NMR spectroscopy for a lamella structure in an alanine–glycine copolypeptide: a model for the crystalline domain of *Bombyx mori* silk fiber, Protein Sci. 14 (2005) 2654–2657.
[11] S. Keten, M.J. Buehler, Nanostructure and molecular mechanics of spider dragline silk protein assemblies, J. R. Soc. Interface 7 (2010) 1709–1721.
[12] G. Bratzel, M.J. Buehler, Molecular mechanics of silk nanostructures under varied mechanical loading, Biopolymers 97 (2012) 408–417.
[13] J.-N. Wang, S.-Q. Yan, C.-D. Lu, L. Bai, Biosynthesis and characterization of typical fibroin crystalline polypeptides of silkworm *Bombyx mori*, Mater. Sci. Eng. 29 (2009) 1321–1325.
[14] T. Asakura, K. Suita, T. Kameda, S. Afonin, A.S. Ulrich, Structural role of tyrosine in *Bombyx mori* silk fibroin, studied by solid-state NMR and molecular mechanics on a model peptide prepared as silk I and II, Magn. Reson. Chem. 42 (2004) 258–266.
[15] T. Yamane, K. Umemura, T. Asakura, The structural characteristics of *Bombyx mori* silk fibroin before spinning as studied with molecular dynamics simulation, Macromolecules 35 (2002) 8831–8838.
[16] P. Taddei, P. Monti, Vibrational infrared conformational studies of model peptides representing the semicrystalline domains of *Bombyx mori* silk fibroin, Biopolymers 78 (2005) 249–258.
[17] Y.-B. Deng, J.-H. Cai, P. Zhou, Naturally stable free radical in the silk fibroin and its structure environment studied by EPR and DFT, Spectrosc. Lett. 45 (2012) 285–295.
[18] J.J.P. Stewart, Application of the PM6 method to modeling proteins, J. Mol. Model. 15 (2009) 765–805.
[19] K. Tsemekhman, L. Goldschmidt, D. Eisenberg, D. Baker, Cooperative Hydrogen Bonding in Amyloid Formation, 2007. 761–764, http://dx.doi.org/10.1110/ps.062609607.
[20] V. Horváth, Z. Varga, A. Kovács, Substituent effects on long-range interactions in the β-sheet structure of oligopeptides, J. Mol. Struct. THEOCHEM 755 (2005) 247–251.
[21] V. Horváth, Z. Varga, A. Kovács, Long-Range effects in oligopeptides. A theoretical study of the β-sheet structure of Gly n(n = 2–10), J. Phys. Chem. A108 (2004) 6869–6873.

[22] Y.-L. Zhao, Y.-D. Wu, A theoretical study of beta-sheet models: is the formation of hydrogen-bond networks cooperative? J. Am. Chem. Soc. 124 (2002) 1570–1571.
[23] R. Wieczorek, J.J. Dannenberg, H-bonding cooperativity and energetics of alpha-helix formation of five 17-amino acid peptides, J. Am. Chem. Soc. 125 (2003) 8124–8129.
[24] G. Rossetti, A. Magistrato, A. Pastore, P. Carloni, Hydrogen bonding cooperativity in polyQ beta-sheets from first principle calculations, J. Chem. Theory Comput. 6 (2010) 1777–1782.
[25] F. Tofoleanu, N.-V. Buchete, Alzheimer's Aβ peptide interactions with lipid membranes: fibrils, oligomers and polymorphic amyloid channels, Prion 6 (2012) 339–345.
[26] A. Lupan, A.-Z. Kun, F. Carrascoza, R. Silaghi-Dumitrescu, Performance comparison of computational methods for modeling alpha-helical structures, J. Mol. Model. 19 (2013) 193–203.
[27] Wavefunction, I., Spartan, 2006.
[28] M. Korth, M. Pitonák, J. Řezáč, P. Hobza, A transferable H-bonding correction for semiempirical, J. Chem. Theory Comput. 6 (2010) 344–352.
[29] A. Klamt, G. Schüürmann, COSMO: a new approach to dielectric screening in solvents with explicit expressions for the screening energy and its gradient, J. Chem. Soc. Perkin Trans. 2 (799) (1993), http://dx.doi.org/10.1039/p29930000799.
[30] J.J.P. Stewart, Optimization of parameters for semiempirical methods V: modification of NDDO approximations and application to 70 elements, J. Mol. Model. 13 (2007) 1173–1213.
[31] J.J. Stewart, MOPAC: a semiempirical molecular orbital program, J. Comput. Aided Mol. Des. 4 (1990) 1–105.
[32] A. Kun, A. Lupan, S.-D. R., PM6 modeling of alpha helical polypeptide structures, Studia 55 (2010) 265–275.
[33] Y. Zhao, D.G. Truhlar, Density functionals with broad applicability in chemistry, Acc. Chem. Res. 41 (2008) 157–167.
[34] M.J. Frisch, et al., Gaussian 09, Revision A.02, 2009.
[35] B. Brooks, R. Bruccoleri, CHARMM: a program for macromolecular energy, minimization, and dynamics calculations, J. Comput. Chem. 4 (1983) 187–217.
[36] A.D. MacKerell, et al., All-atom empirical potential for molecular modeling and dynamics studies of proteins †, J. Phys. Chem. B102 (1998) 3586–3616.
[37] Hypercube, Inc., HyperChem, 2007.
[38] J.P. Ryckaert, G. Ciccotti, H.J.C. Berendsen, Numerical-integration of Cartesian equations of motion of a system with constraints-molecular-dynamics of N-alkanes, J. Comput. Phys. 23 (1977) 327–341.
[39] R. Salomon-Ferrer, D.A. Case, R.C. Walker, An overview of the Amber biomolecular simulation package, Wiley Interdiscip. Rev. Comput. Mol. Sci. 3 (2013) 198–210.